DOI: 10.1002/cmdc.201200291

Inhibition of Bacterial Dihydrofolate Reductase by 6-Alkyl-2,4-diaminopyrimidines

Baskar Nammalwar,[a] Christina R. Bourne,*[b] Richard A. Bunce,*[a] Nancy Wakeham,[b] Philip C. Bourne,[b] Kal Ramnarayan,[c] Shankari Mylvaganam,[c] K. Darrell Berlin,[a] Esther W. Barrow,[b] and William W. Barrow[b]

(±)-6-Alkyl-2,4-diaminopyrimidine-based inhibitors of bacterial dihydrofolate reductase (DHFR) have been prepared and evaluated for biological potency against *Bacillus anthra*cis and *Staphylococcus aureus*. Biological studies revealed attenuated activity relative to earlier structures lacking substitution at C6 of the diaminopyrimidine moiety, though minimum inhibitory concentration (MIC) values are in the 0.125–8 μg mL^{-1} range for both organisms. This effect was rationalized from three-dimensional X-ray structure studies that indicate the presence of a side pocket containing two water molecules adjacent to the main binding pocket. Because of the hydrophobic nature of the substitutions at C6, the main interactions are with protein residues Leu 20 and Leu 28. These interactions lead to a minor conformational change in the protein, which opens the pocket containing these water molecules such that it becomes continuous with the main binding pocket. These water molecules are reported to play a critical role in the catalytic reaction, highlighting a new area for inhibitor expansion within the limited architectural variation at the catalytic site of bacterial DHFR.

Introduction

It is well known that the arsenal of available antibiotics is not sufficient to meet the growing burden of bacterial resistance and that fewer efforts are being made at a pharmaceutical level to pursue new substances with antibiotic properties.[1–3] We have combined this need with that of biodefense in repurposing the antifolate target dihydrofolate reductase (DHFR, EC.1.5.1.3). Our recently reported library of dihydrophthalazine-containing compounds has demonstrated potency against DHFR in *Bacillus anthracis*.[4–6] We are also monitoring the broad-spectrum potency of this series, and in particular, looking for anti-staphylococcal activity. *Staphylococcus aureus* is a prominent human pathogen with increasing antibiotic resistance, such as methillicin- and vancomycin-resistant forms (MRSA and VRSA, respectively).[7,8] Previous work from our group demonstrated a conserved potency of our initial compound RAB1 (**1a**) against *S. aureus* 29213, four MRSA strains and three VRSA strains.[9] Compound **1b** was also found to be highly active. We have now attempted to enhance the broad-spectrum potency of this series by making use of molecular modeling techniques interfaced with chemistry, microbiology and biochemistry, and X-ray crystallography.

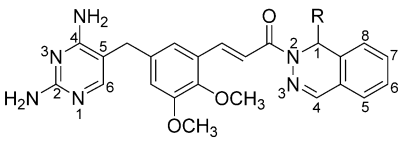

(±)-**1a** (R = $CH_2CH_2CH_3$; RAB1)
(±)-**1b** (R = $CH{=}C(CH_3)_2$)

The previously determined *B. anthracis* DHFR co-crystal structure in complex with **1a** revealed a preference for the *S*-enantiomer at the single chiral center bearing a propyl moiety.[5] This is in contrast to the co-crystal structure of *S. aureus* DHFR with **1a**, which revealed an alternate position for the dihydrophthalazine portion of the inhibitor containing the chiral center. Binding limited one position to the *S*-enantiomer, while the alternate position residing in a shallow surface pocket could accommodate either enantiomer.[9] The binding site residues in contact with RAB1 (**1a**) show little variation in sequence identity between the *S. aureus* and *B. anthracis* species.[5,10] However, the shape of the binding site in *S. aureus* DHFR is generally wider than that of *B. anthracis* DHFR, allowing formation of the secondary binding surface, which we observed to be influenced by residue changes on the periphery of the site. These changes include a loss of an aromatic stacking interaction with Phe 151 due to a His residue at position 30 in contrast to a Phe or Tyr, as well as loss of electrostatic stabilization arising from Tyr to Phe changes at residues 47 and 68.[10] These observations highlighted how residues from out-

[a] Dr. B. Nammalwar, Prof. R. A. Bunce, Prof. K. D. Berlin
Department of Chemistry, Oklahoma State University
Stillwater, OK 74078 (USA)
E-mail: rab@okstate.edu

[b] Dr. C. R. Bourne, Dr. N. Wakeham, Dr. P. C. Bourne, Dr. E. W. Barrow, Prof. W. W. Barrow
Department of Veterinary Pathobiology, Oklahoma State University
Stillwater, OK 74078 (USA)
E-mail: christina.bourne@okstate.edu

[c] Dr. K. Ramnarayan, Dr. S. Mylvaganam
Sapient Discovery Technologies
10929 Technology Place, San Diego, CA 92127 (USA)

side of the binding pocket could modulate interactions and, in this case, allow either enantiomer to be bound in *S. aureus* DHFR versus just the *S*-enantiomer as complexed with *B. anthracis* DHFR.[5]

Despite these differences between the bacterial species, the diaminopyrimidine (DAP) moiety, which is well conserved among anti-DHFR inhibitors, complexes the equivalent protein side chains within the binding site.[5,10] The arrangement of hydrogen-bond participants around the DAP ring allows for precise placement amid surrounding amino acid side chains and requires participation of both the side chain and the main chain from the protein, regardless of species. Examination of the structures of *B. anthracis* and *S. aureus* DHFR highlighted a small unoccupied pocket of ~50 Å^3 adjacent to the C6 position of the DAP ring (Figure 1). In efforts to explore the potential occupancy of this pocket, a series of DAP-based antifolates bearing methyl, ethyl, and propyl groups at C6 of the DAP moiety were designed, synthesized, and evaluated for potency against bacterial DHFR. A similar approach has been reported for the antimalarial compound pyrimethamine, which has poor antibacterial activity due to differences in the plasmodial and bacterial DHFR protein sequences,[10,11] as well as a series of antibacterial propargyl-linked DHFR inhibitors.[12]

Results and Discussion

Chemistry

The synthetic strategy started with 5-iodovanillin (**2**), which led to compounds **3**–**8**, and with **9**, which gave (±)-**10** (Scheme 1). Compounds **8** and (±)-**10a–b** were then coupled to generate racemic **11a–c** and **12a–c** (Scheme 2).

Since both **1a** and **1b** demonstrated excellent inhibitory properties in our previous studies,[5,6] the propyl- and isobutenyl-substituted compounds **11a–c** and **12a–c** were targeted. The synthesis of DAP derivatives **8a–c** involved a seven-step sequence from commercially available 5-iodovanillin (**2**). Methylation of the phenolic hydroxy in **2**, using potassium carbonate and dimethyl sulfate in *N*,*N*-dimethylformamide (DMF), fur-

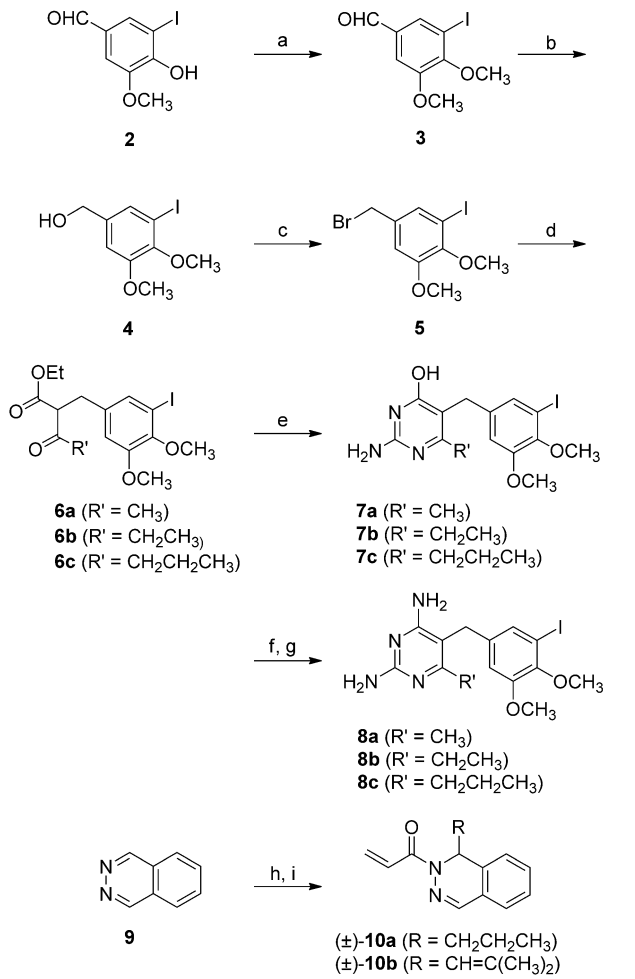

Scheme 1. Synthesis of **8a–c** and **10a–b**. *Reagents and conditions*: a) $(CH_3O)_2SO_2$, K_2CO_3, DMF, 100 °C, 96% yield; b) $NaBH_4$, THF, 23 °C, 99% yield; c) PBr_3, Et_2O, 23 °C, 96% yield; d) $RCOCH_2CO_2Et$, NaOMe, EtOH, 78 °C, [a: R′ = CH_3, b: R′ = CH_2CH_3, c: R′ = $CH_2CH_2CH_3$], 60–68% yield; e) [H_2N=$C(NH_2)_2]_2CO_3$, EtOH, 78 °C, 75–80% yield; f) $POCl_3$, 106 °C; g) NH_3, EtOH, 165 °C, 72–75% yield (two steps); h) RMgBr, THF, 50 °C [a: R = $CH_2CH_2CH_3$, b: R = CH=$C(CH_3)_2$]; i) CH_2=CHCOCl, Et_3N, THF, 0 °C, 40–50% yield (two steps).

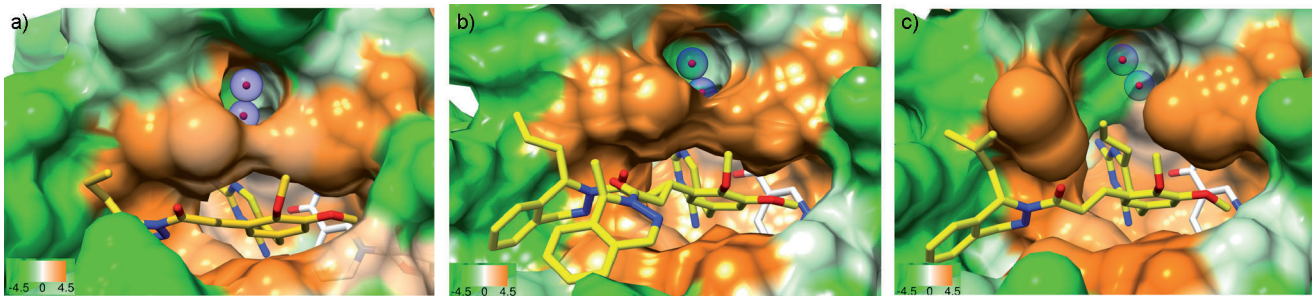

Figure 1. A pocket adjacent to the diaminopyrimidine (DAP) moiety is present in bacterial dihydrofolate reductase (DHFR) proteins and is occupied by two water molecules. Surface renderings of the DHFR protein from a) *B. anthracis* and b) *S. aureus*, both with compound **1a**,[5,10] and c) *S. aureus* complexed with compound **12c**. Surfaces are colored based on Kyte–Doolittle hydrophobicity calculations, where orange is hydrophobic and green is polar. The pocket of interest is continuous with the substrate site only at the DAP ring position; above this, it is gated by opposing Leu residues (20 and 28). In panel c, the movement of Leu 28 results in a complete opening of this pocket with the substrate binding site. In panel b, the alternate position for the dihydrophthalazine moiety of **1a** is shown. In all panels, the position of the co-factor NADPH can be seen at the bottom of the substrate site and, in this view, to the right of it; NADPH is not involved in the pocket or interactions with the alkyl substituents.

nished iododimethoxybenzaldehyde **3**. Further conversion of **3** by reduction with sodium borohydride gave alcohol **4**, and treatment with phosphorus tribromide produced bromide **5**. Reaction of **5** with a series of β-keto esters, in the presence of sodium methoxide in ethanol, led to the benzyl-substituted keto esters **6a–c**. Cyclization of **6a–c** was accomplished in good yields using guanidine carbonate in boiling ethanol to give hydroxypyrimidines **7a–c**, which were used directly in the next sequence. These 4-hydroxypyrimidines were converted to diaminopyrimidines **8a–c** in two steps by refluxing the former in phosphorus oxychloride, followed by treatment with ethanolic ammonia at 165 °C. A similar strategy has been reported previously[13] but did not involve an iodine-substituted substrate. In the current work, this sequence proceeded cleanly to give **8a–c** in 80–91% yields (see Scheme 1).

The dihydrophthalazine coupling partners (±)-**10a–b** were obtained by reacting phthalazine (**9**) with the propyl and isobutenyl Grignard reagents, followed by N-acylation with acryloyl chloride in the presence of triethylamine as described in earlier reports.[5,6]

Final coupling reactions involving **8a–c** and **10a–b** were accomplished using a palladium acetate-promoted Heck coupling in the presence of *N*-ethylpiperidine in anhydrous DMF at 140 °C (see Scheme 2). Purification of the products by flash chromatography, followed by recrystallization, afforded the final racemic compounds **11a–c** and **12a–c** in yields ranging from 78–85%. Spectral and elemental analyses of these materials revealed that each existed as a solvate of water and/or ethanol.

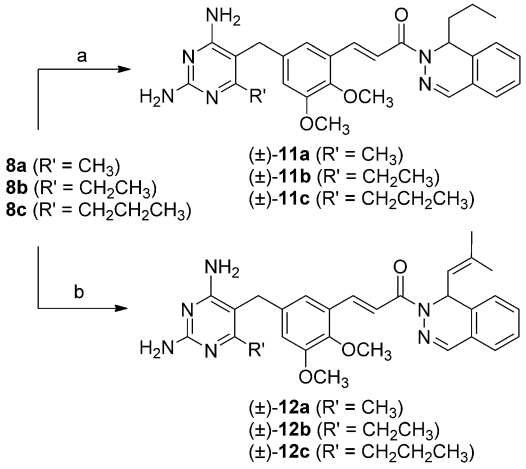

Scheme 2. Synthesis of **11a–c** and **12a–c**. *Reagents and conditions*: a) (±)-**10a**, $Pd(OAc)_2$, *N*-ethylpiperidine, DMF, 140 °C, 81–84% yield; b) (±)-**10b**, $Pd(OAc)_2$, *N*-ethylpiperidine, DMF, 140 °C, 78–84% yield

Biological Activity

Assessment of the parent compounds and inhibitors with alkyl substituents at C6 of the DAP moiety were carried out with purified DHFR in an enzyme assay to gauge the level of effectiveness at competing with the endogenous substrate, dihydrofolic acid. The resulting IC_{50} values were incorporated with the enzyme K_m value for the substrate in order to calculate a K_i value,[14] allowing for direct comparison despite the different enzymatic efficiencies of *B. anthracis* DHFR and *S. aureus* DHFR (Table 1). A general trend of more potent anti-staphylococcal activity was maintained with K_i values generally four-times lower for *S. aureus* than for *B. anthracis*. Substitutions at the C6 position of DAP increased the K_i value for each species, marking them as less effective inhibitors than the parent compounds, and a decrease in potency (higher K_i) was progressive with substitution length. In some instances, the limits of solubility precluded determination of the IC_{50} value (such as with **11b**, **11c** and **12c**), and values are listed as greater than the highest concentration tested.

Table 1. Biological activity of 6-alkyl-DAP inhibitors against bacterial strains *B. anthracis* Sterne and *S. aureus* 29213.

Compd	K_i [nM] (SEM)[a]		MIC [μg mL^{-1}][b]	
	B. anthracis Sterne	*S. aureus* 29213	*B. anthracis* Sterne	*S. aureus* 29213
1a	9.4 (0.2)	1.2 (0.1)	1	0.125–0.25
11a	72.4 (0.6)	4.5 (0.1)	8	0.5
11b	>2400	3.6 (0.1)	4	0.5–2
11c	>2400	4.0 (0.1)	1	1–2
1b	8.3 (0.2)	1.8 (0.1)	0.5	0.125–0.25
12a	14.3 (0.2)	3.4 (0.1)	4	0.25–0.5
12b	25.4 (0.8)	2.9 (0.1)	4	0.25–0.5
12c	>2500	4.1 (0.1)	2	2

[a] The K_i value is calculated from IC_{50} measurements with compensatory weight based on the K_m value for the dihydrofolate substrate. These values are listed with the standard error of the mean (SEM) and represent the mean of three or more experiments. [b] The minimum inhibitory concentration (MIC) is the concentration of inhibitor needed to stop all bacterial growth under the defined conditions (range of values, $n=4$).

These compounds were also incubated in cultures of the two bacterial organisms to determine the minimum inhibitory concentration (MIC) required to inhibit bacterial growth (Table 1), which is a useful parameter for consideration in clinical applications. The MIC values for *S. aureus* progressively increased 10-fold between parent (**1a** and **1b**) versus the C6 propyl substitution (**11c** and **12c**), indicating decreased potency within the cellular system. Interestingly, for *B. anthracis*, the MIC values follow the same trend of progressively decreasing potency only for the compounds bearing an isobutenyl at the chiral center (**1b**, **12a–c**), which is 9 Å from the C6 position. The other series, containing a propyl at the chiral center, displays the same MIC value and thus potent inhibition for the parent (**1a**) as for the C6 propyl substitution **11c**. However, the two intermediate substitutions, **11a** and **11b**, show an increase in MIC value in excess of any expected experimental variation. This is difficult to rationalize in terms of structural elements as the K_i values do not reflect the same trend. Since the MIC measurements are in the context of whole cells, they require the compounds to cross cell membranes, and there are additional factors in the MIC assay that are absent in the K_i measurements. These factors clearly influence the resulting activity, and consequently another explanation could involve cross-reactivity with other member enzymes of the folate pathway, although this has not been demonstrated.

X-ray Data

X-ray crystallography was used to visualize the DAP modifications within the binding site of *S. aureus* DHFR for complexes with **12b** and **12c** (Table 2). Similar experiments with *B. anthracis* DHFR were not successful, as this protein has been observed to crystallize poorly or not at all in the absence of a tightly bound compound in the substrate site (unpublished observation). Due to the high degree of similarity of residues for each DHFR involved in binding, it is feasible to analyze the *S. aureus* DHFR co-crystal structure to draw generalizations about the mode of binding. The resulting electron density maps, obtained prior to crystallographic refinement with the inhibitor, clearly show the positions of the appended atoms on the DAP ring within the *S. aureus* DHFR binding site (Figure 2a,b). For either **12b** or **12c**, the placement within the pocket is as expected, and contacts are conserved from those previously visualized with **1a**.[9] However, the substitutions at C6 complex along the hydrophobic edge of the identified pocket (Figure 1c). These did not protrude into the adjacent 50 Å^3 pocket, where two highly conserved water molecules are located.

Other computational and experimental studies have demonstrated the important role of water at so-called "hydration sites" in protein–ligand binding, analogous to the currently identified water molecules.[15] Calculated energetics indicate the liberation of these two water molecules would require ~4 kcal mol^{-1}; this inhibitor series generally displays binding energies of 42–44 kcal mol^{-1} and are derived largely from van der Waals interactions. These highly conserved water molecules have been seen in previous DHFR structures and are well characterized within the *E. coli* system. Such, water molecules are required for positioning the folate substrate relative to the nicotinamide co-factor, in addition to coordinating the critical catalytic residue Asp 27 to maintain optimum reaction geometry.[16,17] Trp 22 is a secondary residue that also coordinates the water molecules, and it is not clear whether its role is strictly geometric or if it assists in perturbation of the local pK_a as needed to promote protonation of the substrate via Asp 27. It is also suggested that these two conserved waters might provide the catalytic proton, supporting their invariant positions among all DHFR structures known to date and their importance to the protein structure.

The C6 alkyl group on each structure is sandwiched between the face of the central dimethoxybenzene ring of the inhibitor, residues Leu 20, Asp 27 and Leu 28, and the two highly conserved water molecules (Figure 2c,d). In addition, for the **12c** complex, a rotameric change in side chain position of Leu 28 is necessary to accommodate the inhibitor (Figure 1c). As a consequence, this movement alters the position of the distal end of the inhibitor by ~0.7 Å. The energetic costs of this different arrangement likely play a role in the decreased potency. Differences in biological activity between the two species probably arise due to structural elements that influence positioning at the opposite end of the inhibitor (the dihydrophthalazine containing the chiral center, ~9 Å away). Therefore, when relating these observations to the *B. anthracis* DHFR protein, the same mode of binding is expected, including the maintenance of the two water molecules within the pocket. Overall, these observations highlight the relative ease in reordering hydrophobic interactions, which are not dependent on the direction of atomic interactions, rather than displacing the specific hydrogen bonds mediated by the water molecules. Furthermore, the rotameric movement of Leu 28 in the complex with **12c** revealed a continuous opening of the pocket adjacent to the inhibitor binding pocket (Figure 1c). This could prove very advantageous for further inhibitor design and defines a minimum alkyl chain length to achieve this result.

Table 2. Statistics for macromolecular X-ray data collection and refinement of *S. aureus* DHFR + NADPH co-crystallized with compounds (±)-**12b**,**c**.

	(±)-**12b**	(±)-**12c**
PDB code[a]	4FGH	4FGG
Data Collection		
Space Group	$P6_122$	$P6_122$
Cell dimensions		
a, *b*, *c* [Å]	78.9, 78.9, 106.2	79.0, 79.0, 107.5
α, β, γ [°]	90, 90, 120	90, 90, 120
Resolution [Å]	Inf - 2.50 (2.55–2.50)	Inf - 2.30 (2.36–2.30)
R_{int}	16.0 (48.4)	14.4 (50.4)
$I/\sigma I$	19.6 (5.5)	22.8 (4.8)
Completeness [%]	100 (100)	100 (100)
Redundancy	36.0 (26.0)	34.6 (23.6)
Mosaicity	0.74	0.66
Wilson B-factor	34.0	24.8
Refinement		
Resolution [Å]	68.4–2.5	68.4–2.3
R_{work}/R_{free}	19.2/24.6	19.7/24.5
Protein atoms	1324	1330
Ligand/NADPH atoms	39/48	40/48
Water atoms	69	143
B factor, protein	23.5	17.4
B factor, Ligand/NADPH	32.7/24.2	26.6/14.4
B factor, water	30.1	24.1
R.M.S.D. bond lengths [Å]	0.008	0.008
R.M.S.D. bond angles [°]	1.184	1.225

[a] The structures have been deposited in the RCSB Protein Data Bank (PDB) and are available from www.rcsb.org.

Conclusions

Alkyl extensions have been appended to the DAP moiety of propyl- and isobutenyl-substituted, dihydrophthalazine-based DHFR inhibitors, and the activities of the resultant compounds have been evaluated. Testing the potency against *B. anthracis*, a known bioterrorism agent, and *S. aureus*, a prominent human pathogen, revealed modestly decreased potency versus systems lacking substitution at C6 on the pyrimidine. This effect is rationalized based on the three-dimensional structures, which highlight the conservation of two water molecules within a small protein cavity adjacent to the main binding site.

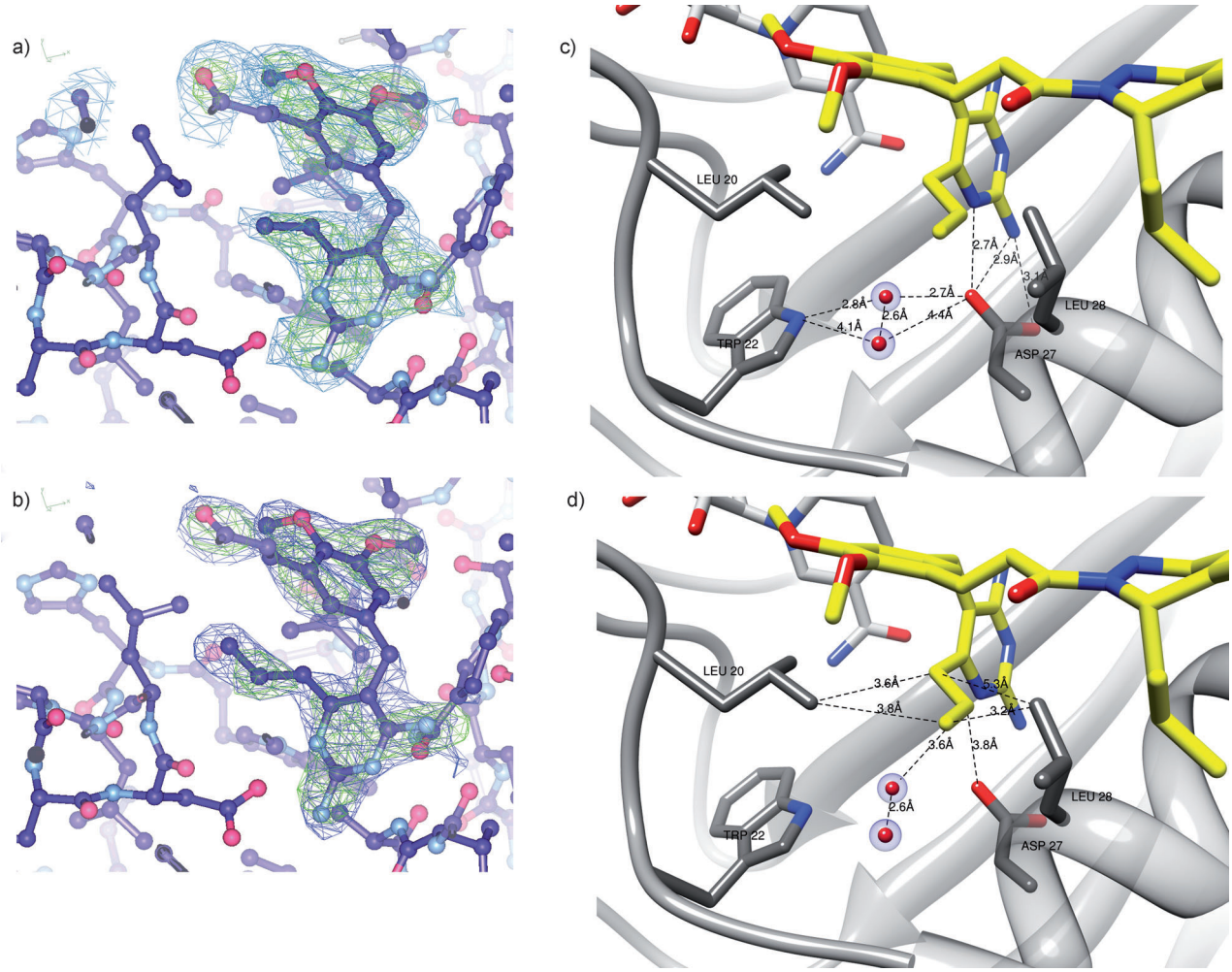

Figure 2. Position and interactions of 6-alkyl substitutions within the binding site of *S. aureus* DHFR. The electron densities for inhibitors a) **12b** and b) **12c**, prior to crystallographic refinement with ligand in place, is depicted. Protein and ligand are shown as ball-and-stick models. Electron density is rendered as mesh with a 2Fo–Fc (blue) map at 1.2 σ and an Fo–Fc (green) map at 3.0 σ. These maps clearly indicate the position of the alkyl extensions in the absence of any model bias. Panels c and d display distance measurements between atoms of inhibitor **12c** (yellow carbon atoms, blue nitrogen atoms and red oxygen atoms) and protein side chains Leu 20, Trp 22, Asp 27, and Leu 28 (colored as **12c** but with grey carbon atoms). The two water molecules discussed in the text are also depicted. The NADPH co-factor is visible behind the inhibitor at the top of the figure; NADPH is not involved in binding at the site of the 6-alkyl extensions.

These water molecules are believed to play a critical role in the catalytic reaction and are not displaced by these inhibitors. The longest extension tested, a propyl group, was the minimum length needed to completely open this side pocket to the main binding site, which may be advantageous in the design of more efficacious agents targeting bacterial DHFR.

Experimental Section

Chemistry

General: Commercial anhydrous *N*,*N*-dimethylformamide (DMF) and dimethyl sulfoxide (DMSO) were stored under dry N_2 and transferred by syringe into reactions when required. Tetrahydrofuran (THF) was dried over KOH pellets and distilled from $LiAlH_4$ prior to use. K_2CO_3 was heated at 120 °C under high vacuum for a period of 16 h and stored in an oven at 90 °C before use. All other commercial reagents were used as received. Unless otherwise specified, all reactions were run under dry N_2 in oven-dried glassware. Reactions were monitored by thin layer chromatography (TLC) on silica gel GF plates (Analtech; cat. no. 21521). Preparative separations were performed by flash column chromatography[18] on silica gel (Davisil grade 62, 60–200 mesh) mixed with UV-active phosphor (Sorbent Technologies; cat. no. UV-05). Band elution for all chromatographic separations was monitored using a hand-held UV lamp. Melting points were recording on a Meltemp apparatus and are uncorrected. IR spectra were run as thin films on NaCl disks using a Varian 800 FT-IR instrument. ^1H and ^{13}C NMR spectra were measured on a Varian GEMINI 300 instrument at 300 MHz (^1H) and 75 MHz (^{13}C), and chemical shifts (δ) are referenced to internal tetramethylsilane (TMS). Elemental analyses were performed by Atlantic Microlab, Inc. (Norcross, USA).

5-Iodo-3,4-dimethoxybenzaldehyde (3): This compound was prepared from **2** on a 0.27 mol scale using the method of Nimgirawath.[19] The crude product was recrystallized (4:1 EtOH/water) to give **3** as a white solid (25.2 g, 96%): mp: 71–72 °C (lit. mp: 71–

72 °C[19]); ^{1}H NMR (300 MHz, $CDCl_3$): δ = 9.83 (s, 1H), 7.85 (d, J = 1.7 Hz, 1H), 7.41 (d, J = 1.7 Hz, 1H), 3.93 (s, 3H), 3.92 ppm (s, 3H); ^{13}C NMR (75 MHz, $CDCl_3$): δ = 189.7, 154.2, 153.0, 134.7, 133.9, 111.0, 92.1, 60.7, 56.1 ppm; IR (NaCl): $\tilde{\nu}$ = 2832, 2730, 2693 cm^{-1}; To the best of our knowledge, no IR or ^{13}C NMR data for **3** have been reported previously.

(3-Iodo-4,5-dimethoxyphenyl)methanol (4): The method of Chowdhury and co-workers was modified.[20] A solution of **3** (25.0 g, 85.0 mmol) in THF (100 mL) was treated portion-wise over 5 min with $NaBH_4$ (1.91 g, 50.0 mmol), and the reaction was stirred at RT for 45 min. The reaction mixture was quenched with saturated aq NH_4Cl (100 mL) and extracted with EtOAc (3×125 mL). The combined organic layers were washed with saturated aq NaCl (100 mL), dried ($MgSO_4$), filtered and concentrated under vacuum to yield **4** as a thick colorless liquid (24.8 g, 99%): ^{1}H NMR (300 MHz, $CDCl_3$): δ = 7.27 (d, J = 1.6 Hz, 1H), 6.86 (d, J = 1.6 Hz, 1H), 4.53 (s, 2H), 3.83 (s, 3H), 3.79 (s, 3H), 2.83 ppm (br s, 1H); ^{13}C NMR (75 MHz, $CDCl_3$): δ = 152.4, 147.7, 139.0, 128.3, 111.2, 92.1, 63.9, 60.3, 55.8 ppm; IR (NaCl): $\tilde{\nu}$ = 3392, 2824 cm^{-1}.

5-(Bromomethyl)-1-iodo-2,3-dimethoxybenzene (5): A stirred solution of **4** (20.0 g, 68.0 mmol) in dry Et_2O (100 mL) was cooled to 0 °C, and PBr_3 (20.2 g, 7.0 mL, 74.8 mmol, 1.1 equiv) was added dropwise over 20 min. After the addition, stirring was continued with warming to 23 °C for an additional 30 min to ensure complete conversion. The reaction mixture was quenched by dropwise addition of saturated aq $NaHCO_3$ (200 mL) over a period of 45 min. [*Note*: Quenching was done slowly to minimize frothing.] The layers were separated, and the aqueous layer was extracted with EtOAc (3×150 mL). The combined EtOAC and Et_2O layers were washed with saturated aq NaCl, dried ($MgSO_4$), filtered and concentrated under vacuum to yield **5** as a pale yellow solid (23.2 g, 96%): mp: 64–65 °C; ^{1}H NMR (300 MHz, $CDCl_3$): δ = 7.37 (d, J = 1.6 Hz, 1H), 6.91 (d, J = 1.6 Hz, 1H), 4.40 (s, 2H), 3.87 (s, 3H), 3.83 ppm (s, 3H); ^{13}C NMR (75 MHz, $CDCl_3$): δ = 152.5, 149.0, 135.4, 130.7, 113.4, 92.2, 60.4, 56.0, 32.3 ppm; IR (NaCl): $\tilde{\nu}$ = 2827 cm^{-1}.

Ethyl 2-(3-iodo-4,5-dimethoxybenzyl)-3-oxobutanoate (6a): The method of Chowdhury and co-workers was modified.[20] A solution of ethyl acetoacetate (8.75 g, 8.57 mL, 67.0 mmol) in dry EtOH (70 mL) was treated with powdered NaOMe (3.63 g, 67.0 mmol), and the reaction mixture was warmed to 50 °C over 30 min. The warm mixture was treated dropwise with **5** (20.0 g, 56.0 mmol, 0.84 equiv), and the reaction was heated at reflux for 18 h. After cooling, the crude product was concentrated under vacuum and purified on a 100 cm × 3 cm silica gel column (1:3 EtOAc/hexane) to give **6a** as a colorless liquid (15.4 g, 68%): ^{1}H NMR (300 MHz, $CDCl_3$): δ = 7.16 (d, J = 1.6 Hz, 1H), 6.71 (d, J = 1.6 Hz, 1H), 4.17 (q, J = 7.3 Hz, 2H), 3.83 (s, 3H), 3.79 (s, 3H), 3.74 (t, J = 7.3 Hz, 1H), 3.06 (m, 2H), 2.23 (s, 3H), 1.25 ppm (t, J = 7.3 Hz, 3H); ^{13}C NMR (75 MHz, $CDCl_3$): δ = 201.9, 168.8, 152.3, 147.5, 136.2, 130.2, 113.5, 92.3, 61.6, 61.1, 60.3, 55.8, 32.9, 29.5, 14.0 ppm; IR (NaCl): $\tilde{\nu}$ = 2828, 1736, 1716 cm^{-1}.

Ethyl 2-(3-iodo-4,5-dimethoxybenzyl)-3-oxopentanoate (6b): This compound was prepared as above using ethyl 3-oxovalerate (9.69 g, 67.0 mmol) in dry EtOH (70 mL), powdered NaOMe (3.63 g, 67.0 mmol), and **5** (20.0 g, 56.0 mmol, 0.84 equiv) to give **6b** as a colorless liquid (14.1 g, 60%): ^{1}H NMR (300 MHz, $CDCl_3$): δ = 7.15 (d, J = 2.0 Hz, 1H), 6.69 (d, J = 2.0 Hz, 1H), 4.16 (q, J = 7.3 Hz, 2H), 3.82 (s, 3H), 3.79 (s, 3H), 3.74 (t, J = 7.3 Hz, 1H), 3.06 (m, 2H), 2.62 (dq, J = 18.1, 7.3 Hz, 1H), 2.39 (dq, J = 18.1, 7.3 Hz, 1H), 1.23 (t, J = 7.3 Hz, 3H), 1.03 ppm (t, J = 7.3 Hz, 3H); ^{13}C NMR (75 MHz, $CDCl_3$): δ = 204.9, 168.9, 152.3, 147.6, 136.4, 130.3, 113.6, 92.3, 61.5, 60.3, 60.1, 55.9, 36.1, 33.2, 14.0, 7.5 ppm; IR (NaCl): $\tilde{\nu}$ = 2823, 1740, 1714 cm^{-1}.

Ethyl 2-(3-iodo-4,5-dimethoxybenzyl)-3-oxohexanoate (6c): This compound was prepared as above using ethyl butyrylacetate (10.6 g, 67.0 mmol) in dry EtOH (70 mL), powdered NaOMe (3.63 g, 67.0 mmol), and **5** (20.0 g, 56.0 mmol, 0.84 equiv) to give **6c** as a colorless liquid (15.6 g, 64%): ^{1}H NMR (300 MHz, $CDCl_3$): δ = 7.15 (d, J = 1.6 Hz, 1H), 6.70 (d, J = 1.6 Hz, 1H), 4.16 (q, J = 7.3 Hz, 2H), 3.82 (s, 3H), 3.79 (s, 3H), 3.74 (t, J = 7.3 Hz, 1H), 3.06 (m, 2H), 2.55 (dt, J = 17.6, 7.3 Hz, 1H), 2.36 (dt, J = 17.6, 7.3 Hz, 1H), 1.56 (sextet, J = 7.3 Hz, 2H), 1.23 (t, J = 7.3 Hz, 3H), 0.86 ppm (t, J = 7.3 Hz, 3H); ^{13}C NMR (75 MHz, $CDCl_3$): δ = 204.2, 168.7, 152.2, 147.5, 136.3, 130.2, 113.5, 92.2, 61.4, 60.3 (2C), 55.8, 44.5, 33.0, 16.7, 14.0, 13.4 ppm; IR (NaCl): $\tilde{\nu}$ = 2824, 1740, 1714 cm^{-1}.

2-Amino-5-(3-iodo-4,5-dimethoxybenzyl)-6-methylpyrimidin-4-ol (7a): A solution of **6a** (10.0 g, 24.6 mmol) in dry EtOH (30 mL) was treated with guanidine carbonate (17.7 g, 98.5 mmol, 4.00 equiv), and the reaction mixture was heated at reflux for 18 h. The EtOH was evaporated to a minimal volume, ice-cold water (50 mL) was added, and the reaction mixture was kept at 0 °C for 30 min to give a white precipitate. The solid was filtered and washed thoroughly with water (100 mL) and Et_2O (50 mL), and then dried under high vacuum for 6 h to give **7a** as a white solid (7.40 g, 75%): mp: 185–186 °C; ^{1}H NMR (300 MHz, DMSO-d6): δ = 7.54 (br s, 1H), 7.08 (s, 1H), 6.97 (s, 1H), 6.58 (br s, 2H), 3.76 (s, 3H), 3.65 (s, 3H), 3.59 (s, 2H), 1.98 ppm (s, 3H); ^{13}C NMR (75 MHz, DMSO-d6): δ = 169.6, 161.0, 158.4, 151.9, 145.9, 141.0, 128.6, 113.3, 108.6, 92.2, 59.7, 55.7, 29.8, 21.3 ppm; IR (NaCl): $\tilde{\nu}$ = 3516–2358, 1654 cm^{-1}.

2-Amino-5-(3-iodo-4,5-dimethoxybenzyl)-6-ethylpyrimidin-4-ol (7b): This compound was prepared as above using **6b** (10.0 g, 23.8 mmol) and guanidine carbonate (17.7 g, 95.2 mmol, 4.00 equiv) in dry EtOH (30 mL) to give **7b** as a white solid (7.70 g, 78%): mp: 190–191 °C; ^{1}H NMR (300 MHz, DMSO-d6): δ = 11.0 (br s, 1H), 7.07 (s, 1H), 6.94 (s, 1H), 6.54 (br s, 2H), 3.76 (s, 3H), 3.65 (s, 3H), 3.61 (s, 2H), 2.35 (q, J = 7.1 Hz, 2H), 1.01 ppm (t, J = 7.1 Hz, 3H); ^{13}C NMR (75 MHz, DMSO-d6): δ = 167.2 (br), 163.8 (br), 153.9, 152.0, 146.2, 140.1, 128.6, 113.3, 109.0, 92.3, 59.8, 55.8, 28.8, 27.2 (br), 12.6 ppm; IR (NaCl): $\tilde{\nu}$ = 3405–2390, 1666 cm^{-1}.

2-Amino-5-(3-iodo-4,5-dimethoxybenzyl)-6-propylpyrimidin-4-ol (7c): This compound was prepared as above using **6c** (10.0 g, 23.0 mmol) and guanidine carbonate (16.6 g, 92.2 mmol, 4.00 equiv) in dry EtOH (30 mL) to give **7c** as a white solid (7.90 g, 80%): mp: 194–195 °C; ^{1}H NMR (300 MHz, DMSO-d6): δ = 7.16 (br s, 1H), 7.08 (s, 1H), 6.95 (s, 1H), 6.71 (br s, 2H), 3.76 (s, 3H), 3.65 (s, 3H), 3.61 (s, 2H), 2.29 (t, J = 7.3 Hz, 2H), 1.45 (sextet, J = 7.3 Hz, 2H), 0.84 ppm (t, J = 7.3 Hz, 3H); ^{13}C NMR (75 MHz, DMSO-d6): δ = 169.0, 164.2, 157.8, 151.9, 145.9, 141.3, 128.7, 113.3, 108.6, 92.2, 59.8, 55.7, 35.9, 29.4, 21.4, 14.0 ppm; IR (NaCl): $\tilde{\nu}$ = 3520–2320, 1654 cm^{-1}.

5-(3-Iodo-4,5-dimethoxybenzyl)-6-methylpyrimidine-2,4-diamine (8a): A mixture of **7a** (6.00 g, 15.0 mmol) in $POCl_3$ (15 mL) was heated at reflux for 2 h. During this time, the suspension gradually became a light brown solution. The solution was cooled in an ice bath for 20 min and was then slowly added dropwise to crushed ice (150 g) with vigorous stirring to give a white precipitate. The solid was filtered under vacuum and washed thoroughly with water (100 mL), 20% EtOH/water (50 mL), and finally with Et_2O (50 mL) to give the corresponding chloride as a white solid (5.70 g, 91%). This product was contaminated with several minor impurities and proved difficult to purify. Thus, it was used directly in the next step.

A stirred suspension of the chloride (5.50 g, 13.1 mmol) in dry EtOH (80 mL) was cooled to 0 °C, and NH_3 gas was bubbled through the solution for 15–20 min. The resulting solution was transferred to a glass-lined 450 mL stainless steel pressure reactor (Paar; no. 4760) and heated to 165 °C for 16 h. The reaction was cooled, and the solvent was evaporated under vacuum. The crude product was purified by flash chromatography on a 70 cm × 3 cm silica gel column (CH_2Cl_2/MeOH/Et_3N 95:5:1) to give **8a** as a white solid (4.21 g, 80%): mp: 236–237 °C; ^{1}H NMR (300 MHz, DMSO-d6): δ = 6.99 (s, 1H), 6.91 (s, 1H), 6.51 (br s, 2H), 6.14 (br s, 2H), 3.77 (s, 3H), 3.69 (s, 2H), 3.65 (s, 3H), 2.08 ppm (s, 3H); ^{13}C NMR (75 MHz, DMSO-d6): δ = 163.3, 159.6, 159.4, 152.0, 146.4, 138.3, 128.3, 113.4, 102.4, 92.6, 59.8, 55.8, 29.2, 20.1 ppm; IR (NaCl): $\tilde{\nu}$ = 3420–2200, 1637 cm^{-1}.

5-(3-Iodo-4,5-dimethoxybenzyl)-6-ethylpyrimidine-2,4-diamine (8b): This compound was prepared as above using **7b** (6.00 g, 14.4 mmol) and 15 mL of $POCl_3$ to give the expected chloride as a tan solid (5.61 g, 90%). A stirred suspension of the chloride (5.50 g, 12.6 mmol) in dry EtOH (80 mL) was cooled to 0 °C, treated with NH_3, and then heated to 165 °C for 16 h. Purification by flash chromatography (CH_2Cl_2/MeOH/Et_3N 95:5:1) gave **8b** as an off-white solid (4.20 g, 80%): mp: 242–243 °C; ^{1}H NMR (300 MHz, DMSO-d6): δ = 6.98 (d, J = 1.6 Hz, 1H), 6.91 (d, J = 1.6 Hz, 1H), 6.57 (br s, 2H), 6.23 (br s, 2H), 3.77 (s, 3H), 3.72 (s, 2H), 3.65 (s, 3H), 2.41 (q, J = 7.7 Hz, 2H), 1.04 ppm (t, J = 7.7 Hz, 3H); ^{13}C NMR (75 MHz, DMSO-d6): δ = 164.1, 163.6, 159.6, 152.0, 146.4, 138.5, 128.3, 113.4, 101.6, 92.5, 59.8, 55.8, 28.8, 25.8, 12.9 ppm; IR (NaCl): $\tilde{\nu}$ = 3460–2200, 1633 cm^{-1}.

5-(3-Iodo-4,5-dimethoxybenzyl)-6-propylpyrimidine-2,4-diamine (8c): This compound was prepared as above using **7c** (6.00 g, 14.0 mmol) and $POCl_3$ (15 mL) to give the expected chloride as a tan solid (5.70 g, 91%). A stirred suspension of the chloride (5.50 g, 12.3 mmol) in dry EtOH (80 mL) was cooled to 0 °C, treated with NH_3, and then heated to 165 °C for 16 h. Purification by flash chromatography (CH_2Cl_2/MeOH/Et_3N 95:5:1) gave **8c** as an off-white solid (4.31 g, 82%): mp: 233–234 °C; ^{1}H NMR (300 MHz, DMSO-d6): δ = 6.98 (s, 1H), 6.91 (s, 1H), 6.39 (br s, 2H), 6.06 (br s, 2H), 3.77 (s, 3H), 3.72 (s, 2H), 3.66 (s, 3H), 2.36 (t, J = 7.1 Hz, 2H), 1.49 (sextet, J = 7.1 Hz, 2H), 0.84 ppm (t, J = 7.1 Hz, 3H); ^{13}C NMR (75 MHz, DMSO-d6): δ = 164.2, 163.4, 160.2, 151.9, 146.3, 138.8, 128.4, 113.4, 101.8, 92.5, 59.8, 55.8, 34.9, 29.0, 21.5, 13.9 ppm; IR (NaCl): $\tilde{\nu}$ = 3480–2340, 1639 cm^{-1}.

(±)-(*E*)-3-{5-[(2,4-Diamino-6-methyl-5-pyrimidinyl)methyl]-2,3-dimethoxyphenyl}-1-(1-propyl-2(1*H*)-phthalazinyl)-2-propen-1-one (11a): A stirred solution of **8a** (1.00 g, 2.50 mmol) in dry DMF (8 mL) under N_2 was treated with (±)-1-(1-propyl-2(1*H*)-phthalazinyl)-2-propen-1-one [(±)-**10a**][6] (627 mg, 2.75 mmol, 1.10 equiv) dissolved in DMF (1 mL), followed by *N*-ethylpiperidine (310 mg, 0.38 mL, 2.75 mmol, 1.10 equiv). This solution was then treated with $Pd(OAc)_2$ (20 mg, 0.089 mmol), and the reaction mixture was heated at 140 °C for 20 h. Isolation of the expected product was achieved by pouring the cooled reaction mixture directly onto a 50 cm × 2.5 cm silica gel flash chromatography column packed in CH_2Cl_2. Impurities were eluted using CH_2Cl_2, and the final product was collected using CH_2Cl_2/MeOH/Et_3N (97:3:1). Evaporation of the solvent gave a pale yellow solid, which was further purified using a 15 cm × 2 cm silica gel column, packed with CH_2Cl_2 and eluted with CH_2Cl_2/MeOH/Et_3N (97:3:1). This second chromatography removed yellow-colored impurities as well as several minor contaminants. Evaporation of the solvent gave **11a** as a light purple solid (1.05 g, 84%): mp: 137–138 °C; ^{1}H NMR (300 MHz, DMSO-d6): δ = 7.94 (s, 1H), 7.84 (d, J = 15.9 Hz, 1H), 7.60 (d, J = 15.9 Hz, 1H), 7.57–7.37 (complex m, 4H), 7.12 (s, 1H), 6.87 (s, 1H), 6.76 (br s, 2H), 6.28 (br s, 2H), 5.84 (t, J = 6.6 Hz, 1H), 3.78 (s, 3H), 3.76 (s, 2H), 3.74 (s, 3H), 2.17 (s, 3H), 1.54 (m, 2H), 1.19 (m, 2H), 1.16 ppm (t, J = 7.1 Hz, 3H); ^{13}C NMR (75 MHz, DMSO-d6): δ = 165.5, 163.5, 158.5, 152.5, 146.0, 142.9, 136.7, 135.9, 133.6, 131.7, 128.3, 127.8, 126.5, 126.1, 123.6, 117.9 (2C), 114.0, 103.1, 60.7, 55.7, 50.3, 22.6, 19.7, 17.8, 15.2, 13.6 ppm (one aromatic C was unresolved); IR (NaCl): $\tilde{\nu}$ = 3329, 3185, 1651, 1616 cm^{-1}; Anal. calcd for $C_{28}H_{32}N_6O_3 \cdot 3.5H_2O \cdot 0.5EtOH$: C 57.60, H 6.33, N 13.88, found: C 57.75, H 6.43, N 13.54.

(±)-(*E*)-3-{5-[(2,4-Diamino-6-ethyl-5-pyrimidinyl)methyl]-2,3-dimethoxyphenyl}-1-(1-propyl-2(1*H*)-phthalazinyl)-2-propen-1-one (11b): This compound was prepared as above using **8b** (1.00 g, 2.42 mmol), (±)-**10a** (606 mg, 2.66 mmol, 1.10 equiv),[6] *N*-ethylpiperidine (300 mg, 0.36 mL, 2.66 mmol, 1.10 equiv), and $Pd(OAc)_2$ (20 mg, 0.089 mmol) dissolved in dry DMF (9 mL) under N_2 to give **11b** as a pale yellow solid (1.06 g, 85%): mp: 192–193 °C; ^{1}H NMR (300 MHz, DMSO-d6): δ = 7.94 (s, 1H), 7.84 (d, J = 15.9 Hz, 1H), 7.61 (d, J = 15.9 Hz, 1H), 7.57–7.36 (complex m, 4H), 7.12 (overlapping s, 2H and 1H), 6.88 (s, 1H), 6.60 (br s, 2H), 5.84 (t, J = 6.6 Hz, 1H), 3.78 (overlapping s, 3H and 2H), 3.74 (s, 3H), 2.52 (obscured, 2H), 1.53 (m, 2H), 1.18 (t, J = 7.1 Hz, 3H), 1.16 (obscured, 2H), 1.10 ppm (t, J = 7.1 Hz, 3H); ^{13}C NMR (75 MHz, DMSO-d6): δ = 165.5, 164.1, 157.4, 152.5, 146.1, 142.9, 136.6, 135.6, 133.6, 131.7, 128.3, 127.9, 126.5, 126.1, 123.6, 118.0, 117.9, 114.0, 102.7, 60.8, 55.8, 50.3, 36.8, 29.0, 24.8, 17.8, 13.6, 12.8 ppm (one aromatic C was unresolved); IR (NaCl): $\tilde{\nu}$ = 3329, 3185, 1651, 1616 cm^{-1}; Anal. calcd for $C_{29}H_{34}N_6O_3 \cdot 5.0H_2O$: C 57.60, H 6.33, N 13.90, found: C 57.67, H 6.33, N 13.61.

(±)-(*E*)-3-{5-[(2,4-Diamino-6-propyl-5-pyrimidinyl)methyl]-2,3-dimethoxyphenyl}-1-(1-propyl-2(1*H*)-phthalazinyl)-2-propen-1-one (11c): This compound was prepared as above using **8c** (1.00 g, 2.34 mmol), (±)-**10a** (587 g, 2.57 mmol, 1.10 equiv),[6] *N*-ethylpiperidine (290 mg, 0.35 mL, 2.57 mmol, 1.10 equiv), and $Pd(OAc)_2$ (20 mg, 0.089 mmol) dissolved in dry DMF (9 mL) under N_2 to give **11c** as an off-white solid (1.00 g, 81%): mp: 140–141 °C; ^{1}H NMR (300 MHz, DMSO-d6): δ = 7.93 (s, 1H), 7.85 (d, J = 15.9 Hz, 1H), 7.58 (d, J = 15.9 Hz, 1H), 7.57–7.35 (complex m, 4H), 7.09 (s, 1H), 6.88 (s, 1H), 6.50 (br s, 2H), 6.09 (br s, 2H), 5.84 (t, J = 6.6 Hz, 1H), 3.77 (overlapping s, 3H and 2H), 3.74 (s, 3H), 2.44 (t, J = 7.1 Hz, 2H), 1.53 (m, 2H), 1.16 (m, 4H), 0.87 (t, J = 7.1 Hz, 3H), 0.82 ppm (t, J = 7.1 Hz, 3H); ^{13}C NMR (75 MHz, DMSO-d6): δ = 165.5, 163.6 (2C), 159.6, 152.4, 145.9, 142.8, 136.6, 136.4, 133.6, 131.7, 128.2, 127.8, 126.5, 126.1, 123.6, 117.9, 117.7, 114.1, 102.4, 60.8, 55.7, 50.3, 36.8, 34.7, 29.5, 21.5, 17.8, 13.9, 13.6 ppm; IR (NaCl): $\tilde{\nu}$ = 3335, 3190, 1650, 1615 cm^{-1}; Anal. calcd for $C_{30}H_{36}N_6O_3 \cdot 2.75H_2O$: C 62.32, H 6.92, N 14.32, found: C 62.26, H 6.69, N 14.06.

(±)-(*E*)-3-{5-[(2,4-Diamino-6-methyl-5-pyrimidinyl)methyl]-2,3-dimethoxyphenyl}-1-(1-isobutenyl-2(1*H*)-phthalazinyl)-2-propen-1-one (12a): This compound was prepared as above using **8a** (1.00 g, 2.50 mmol), (±)-1-(1-isobutenyl-2(1*H*)-phthalazinyl)-2-propen-1-one [(±)-**10b**] (660 mg, 2.75 mmol, 1.10 equiv),[6] *N*-ethylpiperidine (310 mg, 0.38 mL, 2.75 mmol, 1.10 equiv), and $Pd(OAc)_2$ (20 mg, 0.089 mmol) dissolved in dry DMF (9 mL) under N_2 to give **12a** as an off-white solid (1.02 g, 80%): mp: 165–166 °C; ^{1}H NMR (300 MHz, DMSO-d6): δ = 7.93 (s, 1H), 7.83 (d, J = 15.9 Hz, 1H), 7.56 (d, J = 15.9 Hz, 1H), 7.52 (m, 2H), 7.43 (d, J = 7.1 Hz, 1H), 7.30 (d, J = 7.1 Hz, 1H), 7.11 (s, 1H), 6.96 (br s, 2H), 6.86 (s, 1H), 6.52 (br s, 2H), 6.49 (d, J = 9.9 Hz, 1H), 5.24 (d, J = 9.9 Hz, 1H), 3.78 (s, 3H), 3.76 (s, 2H), 3.73 (s, 3H), 2.19 (s, 3H), 1.96 (s, 3H), 1.60 ppm (s, 3H); ^{13}C NMR (75 MHz, DMSO-d6): δ = 165.2, 163.7, 157.8, 152.5, 146.1, 142.1, 136.8, 135.6, 133.8, 133.5, 132.2, 128.2, 127.9, 126.3, 126.2,

123.1, 122.1, 118.0, 117.9, 114.0, 103.3, 60.7, 55.7, 49.2, 29.5, 25.3, 19.1, 18.4 ppm (one aromatic C was unresolved); IR (NaCl): $\tilde{\nu}$ = 3333, 3186, 1652, 1618 cm^{-1}; Anal. calcd for $C_{28}H_{32}N_6O_3 \cdot 2.5H_2O \cdot 0.5EtOH$: C 62.15, H 6.94, N 14.47, found: C 62.44, H 7.04, N 14.60.

(±)-(*E*)-3-{5-[(2,4-Diamino-6-ethyl-5-pyrimidinyl)methyl]-2,3-dimethoxyphenyl}-1-(1-isobutenyl-2(1*H*)-phthalazinyl)-2-propen-1-one (12b): This compound was prepared as above using **8b** (1.00 g, 2.42 mmol), (±)-**10b** (639 mg, 2.66 mmol, 1.10 equiv),[6] *N*-ethylpiperidine (300 mg, 0.36 mL, 2.66 mmol, 1.10 equiv), and $Pd(OAc)_2$ (20 mg, 0.089 mmol) dissolved in dry DMF (9 mL) under N_2 to give **12b** as a pale yellow solid (1.06 g, 84%): mp: 192–193 °C; ^{1}H NMR (300 MHz, DMSO-d6): δ = 7.91 (s, 1H), 7.84 (d, J = 15.9 Hz, 1H), 7.53 (d, J = 15.9 Hz, 1H), 7.50 (m, 2H), 7.43 (d, J = 7.1 Hz, 1H), 7.30 (d, J = 7.1 Hz, 1H), 7.07 (s, 1H), 6.88 (s, 1H), 6.49 (d, J = 9.9 Hz, 1H), 6.29 (br s, 2H), 5.91 (br s, 2H), 5.24 (d, J = 9.9 Hz, 1H), 3.77 (s, 3H), 3.76 (s, 2H), 3.73 (s, 3H), 2.45 (q, J = 7.3 Hz, 2H), 1.96 (s, 3H), 1.60 (s, 3H), 1.07 ppm (t, J = 7.3 Hz, 3H); ^{13}C NMR (75 MHz, DMSO-d6): δ = 166.0, 165.2, 163.4, 160.6, 152.4, 145.9, 142.1, 136.8, 136.7, 133.8, 133.5, 132.2, 128.2, 127.8, 126.3, 126.2, 123.1, 122.2, 117.8, 117.6, 114.1, 101.6, 60.8, 55.7, 49.2, 29.5, 26.4, 25.3, 18.4, 13.0 ppm; IR (NaCl): $\tilde{\nu}$ = 3329, 3182, 1651, 1615 cm^{-1}; Anal. calcd for $C_{30}H_{34}N_6O_3 \cdot 2.0H_2O$: C 64.04, H 6.81, N 14.90, found: C 64.05, H 6.72, N 14.64.

(±)-(*E*)-3-{5-[(2,4-Diamino-6-propyl-5-pyrimidinyl)methyl]-2,3-dimethoxyphenyl}-1-(1-isobutenyl-2(1*H*)-phthalazinyl)-2-propen-1-one (12c): This compound was prepared as above using **8c** (1.00 g, 2.34 mmol), (±)-**10b** (617 mg, 2.57 mmol, 1.10 equiv),[6] *N*-ethylpiperidine (290 mg, 0.35 mL, 2.57 mmol, 1.10 equiv), and $Pd(OAc)_2$ (20 mg, 0.089 mmol) dissolved in dry DMF (9 mL) under N_2 to give **12c** as an off-white solid (980 mg, 78%): mp: 138–139 °C; ^{1}H NMR (300 MHz, DMSO-d6): δ = 7.90 (s, 1H), 7.84 (d, J = 15.9 Hz, 1H), 7.50 (m, 3H), 7.43 (d, J = 7.1 Hz, 1H), 7.30 (d, J = 7.1 Hz, 1H), 7.05 (s, 1H), 6.88 (s, 1H), 6.48 (d, J = 9.9 Hz, 1H), 6.03 (br s, 2H), 5.69 (br s, 2H), 5.24 (d, J = 9.9 Hz, 1H), 3.76 (s, 3H), 3.73 (overlapping s, 2H and 3H), 2.39 (t, J = 7.1 Hz, 2H), 1.95 (s, 3H), 1.59 (s, 3H), 1.52 (sextet, J = 7.1 Hz, 2H), 0.86 ppm (t, J = 7.1 Hz, 3H); ^{13}C NMR (75 MHz, DMSO-d6): δ = 166.4, 165.2, 163.2, 161.4, 152.4, 145.9, 142.1, 137.0, 136.8, 133.8, 133.5, 132.2, 128.2, 127.8, 126.24, 126.17, 123.1, 122.2, 117.8, 117.6, 11.42, 101.8, 60.8, 55.7, 49.2, 35.7, 29.8, 25.3, 21.6, 18.4, 14.1 ppm; IR (NaCl): $\tilde{\nu}$ = 3340, 3177, 1656, 1606 cm^{-1}; Anal. calcd for $C_{31}H_{36}N_6O_3 \cdot 0.75H_2O$: C 66.41, H 7.18, N 14.99, found: C 66.26, H 6.91, N 14.74.

Biology

All biological studies utilized stocks of racemic inhibitor dissolved in DMSO; the concentration of which was kept $\leq$1% during all assay procedures. Enzyme preparation, crystallization, activity (IC_{50} and K_i), and structure solution and refinements were carried out as in previous studies.[6,9]

Briefly, recombinant DHFR protein was expressed in BL21 (DE3) *E. coli* cultures and purified by IMAC using a C-terminal 6-His tag. For crystallization, the 6-His tag was cleaved using an introduced thrombin site, and protein was further purified by size-exclusion chromatography.[9] Crystallization conditions were as previously published: 15% polyethylene glycol 6000 in a 0.1 M 2-(*N*-morpholino)ethanesulfonic acid (MES) buffer (pH 6.5) with 0.15 M NaOAc. The enzymatic activity was assayed using a 0.05 M phosphate buffered system (pH 7.0) also containing 5% glycerol, 10 mM EDTA, 1 mM β-mercaptoethanol at 30 °C with saturating NADPH and dihydrofolate. Conversion of dihydrofolate to tetrahydrofolate was detected with the redox-sensitive tetrazolium dye 3-(4,5-dimethylthiazol-2-yl)-5-(3-carboxymethoxyphenyl)-2-(4-sulfophenyl)-2*H*-tetrazolium (MTS), which was measured by absorbance of 450 nm light. Inhibitors were tested with at least six concentrations, and the percent inhibition relative to a control reaction was used to construct a four-parameter curve fit (KCjunior software package),[21] providing a calculation of the IC_{50} value.

Protocols to determine the minimum inhibitory concentration (MIC) were also described earlier[9] and followed the guidelines given in the Clinical Laboratory and Standards Institute (CLSI) manual.[22] Inhibitors were tested as a series of ten concentrations made in twofold dilutions. The MIC value was defined as the lowest concentration of inhibitor that prevented bacterial growth (visually and as measured at 600 nm) after a 16 h or 20 h incubation at 37 °C in atmospheric CO_2.

X-rax crystallography and modeling

Initial studies utilizing molecular modeling were carried out by Sapient Discovery (San Diego, USA). These included calculation of energy values upon complexation using in-house software based on Monte-Carlo formalism.

X-ray data were collected by Sapient Discovery using a Bruker Proteum/R 6000 instrument suite that included a SMART6000 CCD detector. Data integration and scaling were carried out with the Proteum software suite.[23] Scaling statistics were obtained with XPREP (Table 2). The value for R_{int} as reported from this procedure included all data, in contrast to limiting to the strongest reflections as used in comparable programs.[24] Crystallographic data were isomorphous with the previously determined structure of *S. aureus* DHFR co-crystallized with (±)-**1**,[9] allowing the protein portion of the model (PDB code: 3M08) to be used directly in the refinement program Phenix[25] with visualization and model building using Coot.[26] Figures were generated using the program Chimera.[27] Coordinates and structure factors have been deposited with the Protein Data Bank[28] and were given the identifier codes 4FGH [(±)-**12b**] and 4FGG [(±)-**12c**].

Acknowledgements

We gratefully acknowledge support of this work by the US National Institute of Allergy and Infectious Diseases (NIAID) [1-R01-AI090685-01] of the US National Institutes of Health (NIH) to W.W.B. We are also pleased to acknowledge funding for the Oklahoma Statewide NMR Facility by the National Science Foundation (USA) (BIR-9512269), the Oklahoma State Regents for Higher Education (USA), the W. M. Keck Foundation (Los Angeles, USA), and Conoco, Inc. Molecular graphic images were produced using the UCSF Chimera package from the Resource for Biocomputing, Visualization, and Informatics at the University of California, San Francisco [supported by NIH P41 RR001081].

Keywords: 6-alkylpyrimidines · antibiotics · *Bacillus anthracis* · dihydrofolate reductases · inhibitors · *Staphylococcus aureus*

[1] M. A. Fischbach, C. T. Walsh, *Science* **2009**, *325*, 1089–1093.
[2] B. Hamad, *Nat. Rev. Drug Discovery* **2010**, *9*, 675–676.
[3] L. L. Silver, *Clin. Microbiol. Rev.* **2011**, *24*, 71–109.
[4] E. W. Barrow, J. Dreier, S. Reinelt, P. C. Bourne, W. W. Barrow, *Antimicrob. Agents Chemother.* **2007**, *51*, 4447–4452.

[5] C. B. Bourne, R. A. Bunce, P. C. Bourne, K. D. Berlin, E. W. Barrow, W. W. Barrow, *Antimicrob. Agents Chemother.* **2009**, *53*, 3065 – 3073.
[6] B. Nammalwar, R. A. Bunce, K. D. Berlin, C. R. Bourne, P. C. Bourne, E. W. Barrow, W. W. Barrow, *Eur. J. Med. Chem.* **2012**, *54*, 387 – 396.
[7] J. P. Powell, R. P. Wenzel, *Expert Rev. Anti-infect. Ther.* **2008**, *6*, 299 – 307.
[8] C. Torres, *Nat. Med.* **2010**, *16*, 628 – 631.
[9] C. R. Bourne, E. W. Barrow, R. A. Bunce, P. C. Bourne, K. D. Berlin, W. W. Barrow, *Antimicrob. Agents Chemother.* **2010**, *54*, 3825 – 3833.
[10] L. Adane, P. V. Bharatam, *Curr. Med. Chem.* **2008**, *15*, 1552 – 1569.
[11] D. C. Chan, A. C. Anderson, *Curr. Med. Chem.* **2006**, *13*, 377 – 398.
[12] K. M. Frey, J. Liu, M. N. Lombardo, D. B. Bolstad, D. L. Wright, A. C. Anderson, *J. Mol. Biol.* **2009**, *387*, 1298 – 1308.
[13] a) J. P. Jonak, S. F. Zakrzewski, L. M. Mead, *J. Med. Chem.* **1972**, *15*, 662 – 665; b) B. R. Baker, B. T. Ho, D. V. Santi, *J. Pharm. Sci.* **1965**, *54*, 1415; c) B. Roth, E. Aig, K. Lane, B. S. Rauckman, *J. Med. Chem.* **1980**, *23*, 535 – 541.
[14] C. Yung-Chi, W. H. Prusoff, *Biochem. Pharmacol.* **1973**, *22*, 3099 – 3108.
[15] For overviews on theoretical and empirical observations on the participation of water in binding sites and activation processes, see a) D. J. Huggins, W. Sherman, B. Tidor, *J. Med. Chem.* **2012**, *55*, 1424 – 1444; b) J. Michel, J. Tirado-Rives, W. L. Jorgensen, *J. Am. Chem. Soc.* **2009**, *131*, 15403 – 15411; c) P. Cozzini, M. Fornabaio, A. Marabotti, D. J. Abraham, G. E. Kellogg, A. Mozzarelli, *Curr. Med. Chem.* **2004**, *11*, 3093 – 3118; d) J. E. Ladbury, *Chem. Biol.* **1996**, *3*, 973 – 980.
[16] G. P. Miller, S. J. Benkovic, *Chem. Biol.* **1998**, *5*, R105 – R113.
[17] M. S. Warren, K. A. Brown, M. F. Farnum, E. E. Howell, J. Kraut, *Biochemistry* **1991**, *30*, 11092 – 11103.
[18] W. C. Still, M. Kahn, A. Mitra, *J. Org. Chem.* **1978**, *43*, 2923 – 2925.
[19] S. Nimgirawath, *Aust. J. Chem.* **1994**, *47*, 725 – 731.
[20] S. F. Chowdhury, R. H. Guerrero, R. Brun, L. M. Ruiz-Perez, D. G. Pacanowska, I. H. Gilbert, *J. Enzyme Inhib. Med. Chem.* **2002**, *17*, 293 – 302.
[21] KCjunior Software Package, BioTek, Winooski, VT, USA.
[22] *Performance Standards for Antimicrobial Susceptibility Testing: 19th Informational Supplement*, 8th ed., (M100-S19), Clinical and Laboratory Standards Institute (CLSI), Wayne, PA, USA, **2009**, pp. 1 – 65.
[23] Proteum 2 Software Suite, Bruker AXS Inc., Madison, WI, USA, **2006**.
[24] G. Sheldrick, *XPREP. Space Group Determination and Reciprocal Space Plots*, Siemens Analytical X-ray Instruments, Madison, WI, USA, **1991**.
[25] P. D. Adams, P. V. Afonine, G. Bunkoczi, V. B. Chen, I. W. Davis, N. Echols, J. J. Headd, L. W. Hung, G. J. Kapral, R. W. Grosse-Kunstleve, A. J. McCoy, N. W. Moriarty, R. Oeffner, R. J. Read, D. C. Richardson, J. S. Richardson, T. C. Terwilliger, P. H. Zwart, *Acta Crystallogr. Sect. D* **2010**, *66*, 213 – 221.
[26] P. Emsley, B. Lohkamp, W. G. Scott, K. Cowtan, *Acta Crystallogr. Sect. D* **2010**, *66*, 486 – 501.
[27] E. F. Pettersen, T. D. Goddard, C. C. Huang, G. S. Couch, D. M. Greenblatt, E. C. Meng, T. E. Ferrin, *J. Comput. Chem.* **2004**, *25*, 1605 – 1612.
[28] H. M. Berman, J. Westbrook, Z. Feng, G. Gilliland, T. N. Bhat, H. Weissig, I. N. Shindyalov, P. E. Bourne, *Nucleic Acids Res.* **2000**, *28*, 235 – 242.

Received: June 8, 2012
Published online on ■■ ■■, 0000

*B. Nammalwar, C. R. Bourne,**
R. A. Bunce, N. Wakeham, P. C. Bourne,*
K. Ramnarayan, S. Mylvaganam,
K. D. Berlin, E. W. Barrow, W. W. Barrow

■■ – ■■

Inhibition of Bacterial Dihydrofolate Reductase by 6-Alkyl-2,4-diaminopyrimidines

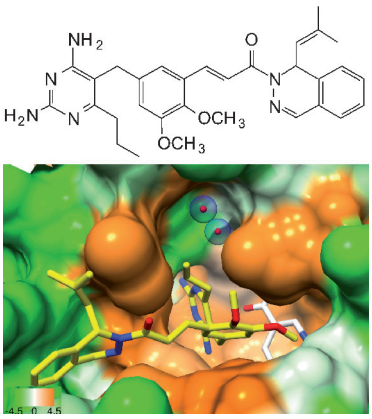

From resistance to terrorism: A series of (±)-6-alkyl-2,4-diaminopyrimidines was synthesized and evaluated for inhibition of bacterial dihydrofolate reductase (DHFR). Biological studies revealed slightly attenuated activity relative to structures lacking C6 alkyl substitution. This arises from a conformational change of the protein resulting in exposure of a hydrated pocket contiguous with the existing binding site.

